# Axonal Neuregulin-1 Regulates Myelin Sheath Thickness

Galin V. Michailov,[1]* Michael W. Sereda,[1,2]*
Bastian G. Brinkmann,[1] Tobias M. Fischer,[4] Bernhard Haug,[3]
Carmen Birchmeier,[5] Lorna Role,[6] Cary Lai,[4] Markus H. Schwab,[1]
Klaus-Armin Nave[1,7]†

In the nervous system of vertebrates, myelination is essential for rapid and accurate impulse conduction. Myelin thickness depends on axon fiber size. We use mutant and transgenic mouse lines to show that axonal Neuregulin-1 (Nrg1) signals information about axon size to Schwann cells. Reduced Nrg1 expression causes hypomyelination and reduced nerve conduction velocity. Neuronal overexpression of Nrg1 induces hypermyelination and demonstrates that Nrg1 type III is the responsible isoform. We suggest a model by which myelin-forming Schwann cells integrate axonal Nrg1 signals as a biochemical measure of axon size.

Myelination requires axonal signals. Millisecond precision is an important aspect of nervous system function (*1*). Myelin sheath thickness, which is one determinant of nerve conduction velocity (*2*), must thus be carefully controlled in development. Nearly 100 years ago, it was observed that the axonal ensheathment is related to axon size (*3*). Myelin thickness is proportional to the diameter of the axon and the internodal length, with only minor species-specific and nerve-specific differences in this ratio (*4–8*). Axon caliber also appears to be a critical determinant of myelination for small axons (*9*). Thus, Schwann cells detect the diameter of the axonal segment that they engulf. This correlation is established during initial development: Peripheral axons with a secondarily reduced diameter have unchanged myelin thickness (*10*).

We have hypothesized that interactions between axonal ligands and glial receptors, such as neuregulins (Nrg) and ErbB receptor tyrosine kinases (*11–14*), can integrate cell surface signals and provide an indirect biochemical measure of the axon caliber.

The *Nrg1* gene encodes more than 15 transmembrane and secreted protein isoforms, generated by alternative promoter usage and mRNA splicing. Nrg1 subtypes I through III share the epidermal growth factor–like signaling domain and are defined by different amino-termini (*11*, *15*). The N-terminal cystein-rich domain (CRD), as found in the sensory and motor neuron-derived factor (SMDF), defines Nrg1 type III, which in embryonic development is responsible for survival of Schwann cell precursors (*16–21*). No such function has been demonstrated for Nrg1 type I [Heregulin (HRG) or acetylcholine receptor–inducing activity (ARIA)] or Nrg1 type II (glial growth factor).

**Neuregulin-1 and ErbB receptors in mature peripheral nerves.** Expression of *Nrg1* and the *ErbB2* and *ErbB3* genes is maintained in the sciatic nerve of adult mice. Nrg1 was immunodetectable (*22*) in axons (Fig. 1A) and detected by in situ hybridization in the dorsal root ganglia (DRG) and in spinal cord motoneurons (*23*, *24*). Similarly, ErbB2 was immunostained in mature Schwann cells and was associated with myelin (Fig. 1B). Moreover, by using polymer-

[1]Department of Neurogenetics, Max Planck Institute of Experimental Medicine, 37075 Göttingen, Germany. [2]Department of Neurology, [3]Department of Clinical Neurophysiology, University of Göttingen, 37075 Göttingen, Germany. [4]Department of Neuropharmacology, Scripps Research Institute, La Jolla, CA 92037, USA. [5]Max Delbrueck Center for Molecular Medicine, 13125 Berlin, Germany. [6]Columbia University, New York, NY 10032, USA. [7]Hertie Institute of Multiple Sclerosis Research, 37075 Göttingen, Germany.

*These authors contributed equally to this work.
†To whom correspondence should be addressed. E-mail: nave@em.mpg.de

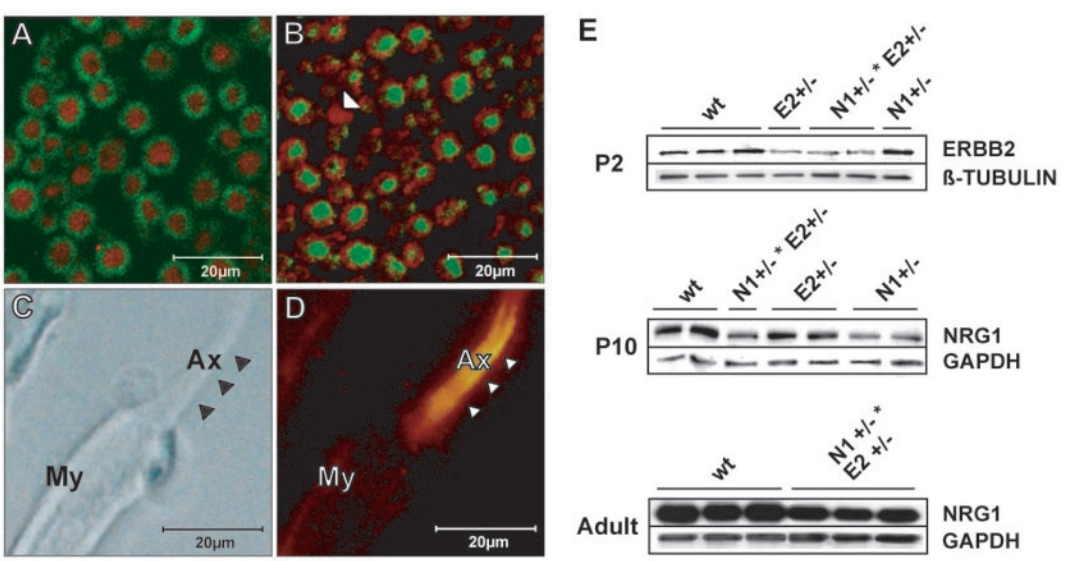


**Fig. 1.** Expression of Nrg1 and ErbB2 in sciatic nerves of adult wild-type and mutant mice (**A**) Confocal image of a normal adult sciatic nerve in cross section. The immunostaining of Nrg1 type III (in red) reveals axonal localization. Myelin is marked with an antibody against myelin P0/MPZ (green). MPZ, myelin protein zero (**B**) Confocal image from another section, immunostained for ErbB2 (in red) and axonal neurofilament (in green). ErbB2 associates with Schwann cells (arrowhead) and the myelin compartment. (**C**) Teased fiber of a sciatic nerve from an adult wild-type (wt) mouse. The phase contrast image reveals a short axonal segment (Ax, arrowheads), stripped of myelin (My) in the course of the preparation. (**D**) Immunostaining of the same fiber shown in (C) with a specific antibody against Nrg1 type III. Nrg1 is rather uniformly distributed along the axonal length (arrowheads). (**E**) Western blot analysis of Nrg1 and ErbB2 in total protein lysates from sciatic nerves, comparing wt animals and mice with reduced gene dosage. (Top) Reduced amount of ErbB2 is obvious in *Nrg1***ErbB2* double heterozygotes ($N1^{+/-}$*$E2^{+/-}$) and in ErbB2 single heterozygotes ($E2^{+/-}$), but not in *Nrg1* heterozygous ($N1^{+/-}$)mice (age P2). A similiar reduction is shown for Nrg1 in sciatic nerves of $N1^{+/-}$*$E2^{+/-}$ and $N1^{+/-}$ (but not in $E2^{+/-}$), analyzed at age P10 (middle) and in the adult (bottom). Probing blots for β-tubulin and glyceraldehyde-3-phosphate dehydrogenase (GAPDH) were used as a loading control.

ase chain reaction (PCR), we could amplify cDNA fragments for ErbB1, ErbB2, and ErbB3 with about equal efficiency from mature sciatic nerves (*24*). Staining of teased-fiber preparations with a Nrg1 type III–specific antibody revealed that the axonal ligand was uniformally distributed along the internode (Fig. 1, C and D).

If Schwann cells obtained information concerning axon size from the steady-state amount of (axon-to-glia) Nrg1 signaling, an experimental reduction in either ligand or receptor number should be perceived by Schwann cells as an apparent "decrease" in axonal caliber. The anticipated reduced amount of myelination would be reflected in an increase in the *g* ratio of the fiber (the numerical ratio between the diameter of the axon proper and the outer diameter of the myelinated fiber). To test this hypothesis, we generated mice with reduced *Nrg1*, *ErbB2*, and/or *ErbB3* gene dosages, obtained by gene targeting (*22*), and produced compound heterozygotes. Whereas the null mutants of these genes die before myelination (*15*, *16*), all compound heterozygotes were fully viable and exhibited normal motor behavior. Peripheral nerves were myelinated and populated with a normal density of Schwann cells (*24*). Sciatic nerves analyzed at different ages [postnatal day 2 (P2), P10, and 6 months] showed steady-state amounts of Nrg1 and glial ErbB2 reduced to half of wild-type amounts (Fig. 1E).

**Reduced neuregulin-1/erbB signaling limits myelination.** The degree of peripheral myelination was also altered. We determined the thickness of sciatic nerve axons and their myelin sheaths for wild-type mice and *Nrg1*ErbB2* compound heterozygtes with the use of light microscopy and digital imaging (*22*) of 0.5-μm semithin cross sections (Fig. 2A). The *g* ratios were calculated from no fewer than 100 myelinated axons per mouse and genotype ($n = 6$). In wild-type mice, the average *g* ratio was 0.68 (±0.032) at P10 and 0.66 (±0.013) at 6 months of age, in agreement with published data (*5*). In contrast, the myelin of compound heterozygotes ($Nrg1^{+/-}$*$ErbB2^{+/-}$) was significantly thinner ($P < 0.001$), both at age P10 ($g = 0.81$) and at 6 months ($g = 0.79$) (fig. S1). The internodal length of sciatic nerve axons was 0.61 ± 0.10 mm in wild-type and 0.64 ± 0.15 in double heterozygous mice (fig. S2), respectively, and the axonal size distribution was also unchanged (Fig. 2, B and C).

All compound heterozygotes were behaviorally normal, but nerve conduction velocity (NCV) was reduced. With the use of the tail nerve of double heterozygotes ($n = 4$), we measured a motor NCV of only 26 ± 1.34 m/s (*22*), in contrast to 34 ± 0.65 m/s in wild-type mice (fig. S3). Current amplitudes were not reduced, and muscle compound action potentials exhibited a normal profile (*24*), bearing no spontaneous electromyogram signals that would be indicative of muscle denervation (*25*).

To determine whether the axonal ligand or the glial receptor was the limiting parameter of myelin thickness, we also analyzed adult mice heterozygous for only the *Nrg1* or the *ErbB2* null allele. Reducing *Nrg1* gene dosage was sufficient to cause the same phenotype as observed in double heterozygotes and even in *Nrg1*ErbB2*ErbB3* triple heterozygotes (Fig. 3A and fig. S4). No decrease in myelin thickness was observed in the $ErbB2^{+/-}$ mice. Thus, under normal conditions, axonal Nrg1 expression appears to serve as a rate-limiting factor for myelination, whereas Schwann cells possess saturating amounts of ErbB receptors. For $Nrg^{+/-}$ mice, the reduction in myelin thickness was more pronounced for small than for large caliber axons (Fig. 3B) but the axonal size distribution did not differ (Fig. 3C).

**Neuregulin-1 overexpression increases myelin thickness.** It is possible that the reduction in myelin thickness in $Nrg1^{+/-}$ mice could be caused by a minor delay in Schwann cell maturation. Moreover, because some Schwann cells express Nrg1 (*26*), its reduction could contribute to hypomyelination. Both hypotheses were tested by cell-specific expression of elevated Nrg1 amounts in axons, beginning in postnatal development. Nrg1 overexpression should mimic an enlarged axonal size from the perspective of the Schwann cells. We generated transgenic mice (*22*) expressing different Nrg1 isoforms under control of the murine Thy 1.2 promotor, which is active in postnatal motoneurons and DRG neurons (*27*), i.e., when most Schwann cells have reached the promyelin stage (*28*). Transgene constructs (Fig. 4A) were derived from murine cDNAs encoding either Nrg1 type I (as present in ARIA/HRG) or Nrg1 type III with an SMDF/CRD domain [we chose the β1a isoforms for each (*11*)]. Microinjection of fertilized mouse oocytes resulted in five transgenic founders, three of which developed mild tremors. Because these mice proved difficult to breed, we included the founders in the analyses at 5 months of age.

We obtained sciatic nerves from three individual Nrg1 type III transgenic founders for biochemical and microscopic analyses. In all transgenics, the overexpression of Nrg1 type III was evident by Western blot analysis when compared with wild-type littermates (Fig. 4B). Morphologically, the peripheral myelin of the adult transgenic mice was thicker than that of controls (Fig. 4C), with some fibers having *g* ratios below 0.4 (lowest was 0.28), a level never observed in wild-type mice. Although the Thy-1.2 promoter is expressed in a mosaic fashion in transgenic mice (*27*), fiber *g* ratios were significantly lower in Nrg1 type III transgenics (*g* ratio of 0.53 ± 0.014) than in nontransgenic littermates (*g* ratio of 0.65 ± 0.014; $P < 0.001$) (fig. S5). Sometimes, normally myelinated axons were in direct proximity to hypermyelinated axons (Fig. 5A), suggesting that

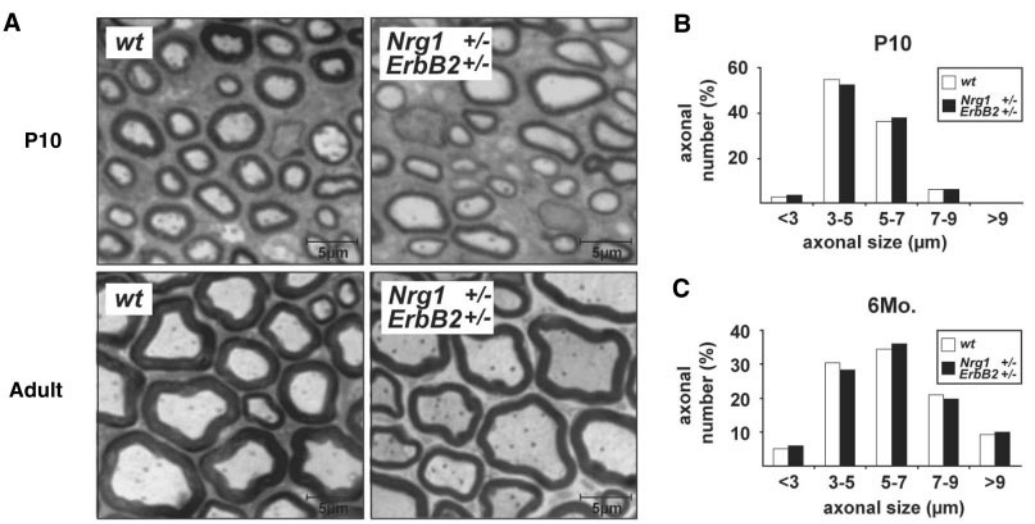


**Fig. 2.** Peripheral nerves of *Nrg1*ErbB2* double heterozygotes are hypomyelinated but exhibit normal axonal size. (**A**) Semithin (0.5 μm) cross sections were prepared from epon-embedded sciatic nerves and stained for myelin. Comparing $Nrg1^{+/-}$*$ErbB2^{+/-}$ (double heterozygotes) with wt controls, reduced myelin thickness was apparent at a young age (P10) and in adults. (**B** and **C**) The distribution of axonal size in sciatic nerves, determined at P10 [in (B)] and at 6 months of age [in (C)], showed no difference between double heterozygotes and controls.

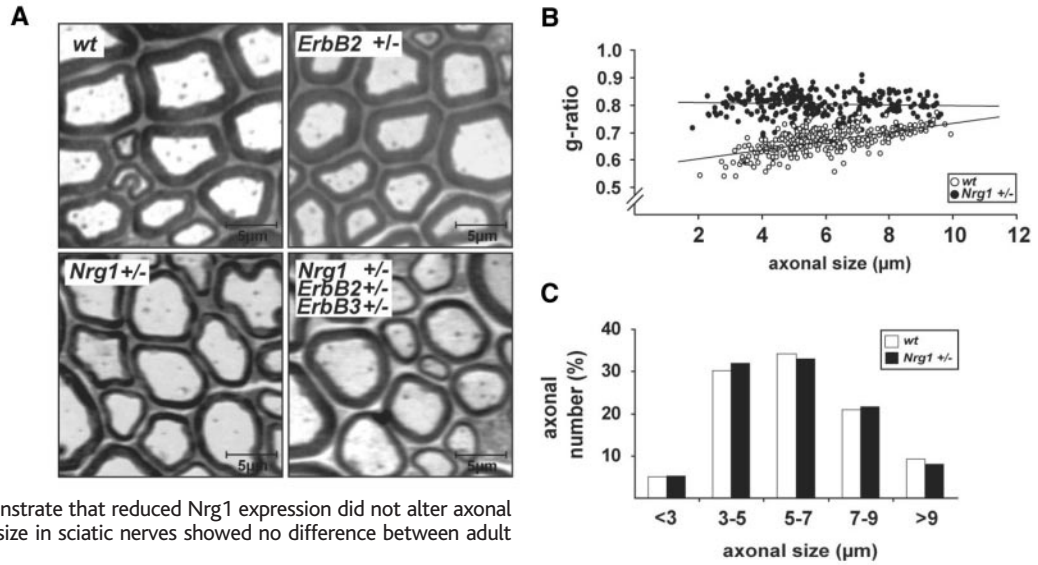


**Fig. 3.** Nrg1 expression amount is a rate-limiting factor for myelination. (**A**) Semithin cross sections (0.5 μm) from an adult sciatic nerve of a wt were compared to sections from age-matched heterozygotes. Hypomyelination, as seen in *Nrg1*$^{+/-}$ mice, is not a feature of *ErbB2*$^{+/-}$ animals. Moreover, triple heterozygotes (*Nrg1*$^{+/-}$**ErbB2*$^{+/-}$**ErbB3*$^{+/-}$) do not differ with respect to peripheral hypomyelination from the *Nrg1*$^{+/-}$ single heterozygote, suggesting that Nrg1 is the limiting factor of myelination. (**B**) After reduced *Nrg1* gene dosage, changes in *g* ratio were observed for nearly all axons but were more pronounced for smaller caliber axons. Scatter plot displays *g* ratios of individual fibers (obtained from three animals) as a function of the respective axon diameter. The data also demonstrate that reduced Nrg1 expression did not alter axonal calibers. (**C**) The distribution of axonal size in sciatic nerves showed no difference between adult *Nrg1* heterozygotes and controls.

these differences reflect mosaic *Thy1.2-Nrg1 type III* transgene expression. The ultrastructure (*22*) and periodicity of the hypermyelinated fibers was normal (Fig. 5B), demonstrating that the increase in myelin thickness was the result of an increase in the number of wrappings. Longitudinal sections revealed that hypermyelination was uniform along the axon and morphologically unrelated to tomacula (*24*).

**Neuregulin-1 type III and myelin growth.** The growth-promoting effect on Schwann cell myelin appeared specific for the Nrg1 type III isoform, because transgenic founder mice overexpressing Nrg1 type I exhibited normal *g* ratios of sciatic nerve fibers (Fig. 4C). Nevertheless, the latter revealed differences in CNS myelin (*29*), suggesting a functional *Nrg1 type I* transgene expression also in these lines. Adult heterozygous mice with reduced *Nrg1 type III* gene dosage (*21*) also possessed abnormally thin myelin, with *g* ratios of 0.77 ± 0.014 (Fig. 4C and fig. S5), similar to those in mice heterozygous for the *Nrg1* null allele. Because the type III–specific knock-out mouse leaves the expression of all other Nrg1 isoforms intact, it is apparent that Nrg1 type I and type II are both unable to functionally compensate for the loss of type III. Although we cannot formally rule out the participation of additional axonal signals and growth factors (*30*), Nrg1 type III emerges as a critical regulator of Schwann cell myelin thickness.

Hypermyelination (reduced *g* ratio) could be mimicked by pathological shrinkage of the axon caliber without altering myelin (*31*). We therefore determined the size distribution of axons in comparable cross sections prepared from adult sciatic nerve (Fig. 5C). This morphometric analysis failed to detect meaningful size differences between *Nrg1* transgenic mice and age-matched controls (Mann-Whitney U test, $P = 0.917$).

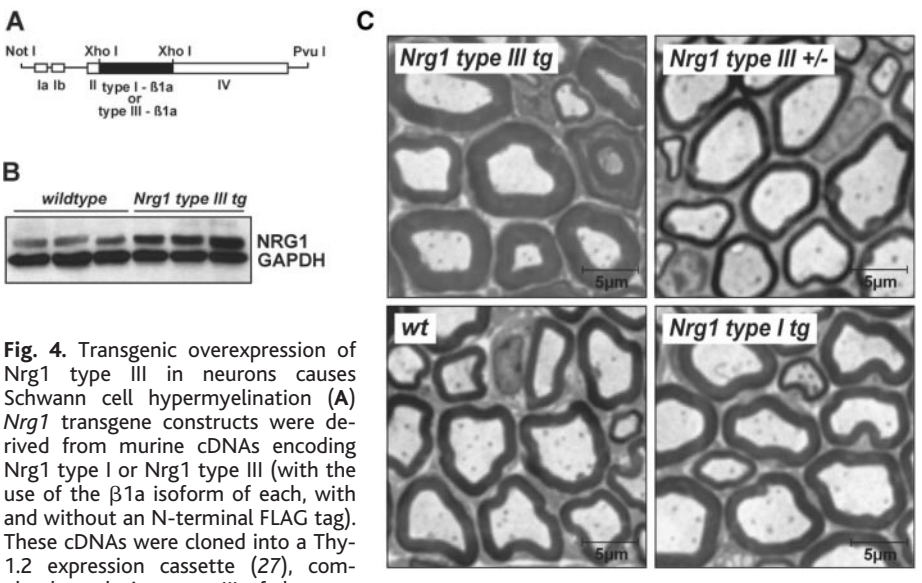


**Fig. 4.** Transgenic overexpression of Nrg1 type III in neurons causes Schwann cell hypermyelination (**A**) *Nrg1* transgene constructs were derived from murine cDNAs encoding Nrg1 type I or Nrg1 type III (with the use of the β1a isoform of each, with and without an N-terminal FLAG tag). These cDNAs were cloned into a Thy-1.2 expression cassette (*27*), completely replacing exon III of the neuronally expressed gene. (**B**) Western blot analysis of sciatic nerve extracts demonstrating overexpression of Nrg1 protein in three different Nrg1 type III founder mice, compared with sciatic nerve extracts from wt littermates. (**C**) Semithin cross sections (0.5 μm) of the sciatic nerve comparing transgenic Nrg1 overexpressing mice with a wt control at age 5 months. Type III transgenics are hypermyelinated (*Nrg1 type III* tg), but not the type I transgenics (*Nrg1 type I* tg). The specific function of Nrg1 type III is confirmed by a corresponding hypomyelination of mice with a type III isoform–specific null allele (*Nrg1 type III*$^{+/-}$).

It was also important to rule out the possibilities that Nrg1 overexpression had changed the absolute number of axons and/or Schwann cells and that hypermyelination was merely the result of a reduced axon:glia ratio. Histology and immunohistochemistry of comparable nerve cross sections revealed no difference in the number of Schwann cell nuclei (240 ± 8 for wild type and 237 ± 23 for *Nrg1 type III* transgenic; $n = 3$) or the number of sciatic nerve axons (3957 ± 19 for wild type and 3883 ± 138 for *Nrg1 type III* transgenic; $n = 3$) (figs. S6 and S7).

Lastly, we calculated the *g* ratios of sciatic nerve fibers from Nrg1-overexpressing mice, plotted as a function of their respective axonal diameters (Fig. 5D). This revealed that hypermyelination was more pronounced for smaller axons than for larger axons. A possible explanation is that a linear increase of axon diameter requires an exponential increase of myelin membrane synthesis (if *g* ratios are maintained constant). Thus, axon size–dependent myelination may well require an exponential increase of neuronal *Nrg1* gene expression as a function of the overall axonal dimension. This regulation is likely not provided for a transgene with the Thy-1.2 promoter.

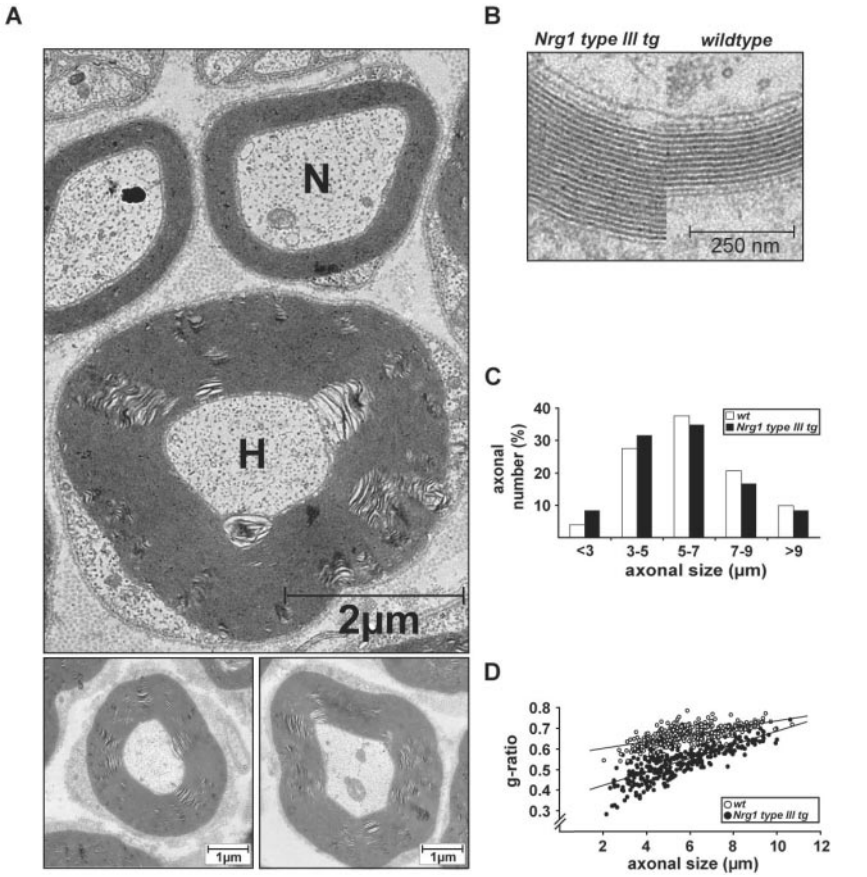


**Fig. 5.** Hypermyelination is dependent on axon size. (**A**) Electron micrographs depicting individual sciatic nerve axons that are hypermyelinated in *Nrg1 type III* transgenic mice. In the top image, a hypermyelinated axon (H) is shown in close proximity to an axon with "normal" myelin (N), possibly derived from a neuron lacking expression of the (Thy1.2 promoter–driven) *Nrg1 type III* transgene. Compact myelin of hypermyelinated axons is prone to fixation artifacts not seen in normally myelinated fibers. (**B**) The ultrastructure and periodicity of compact myelin in hypermyelinated fibers, prepared from *Nrg1 type III* transgenic mice (left), is indistinguishable from myelin prepared from wt mice (right). This demonstrates that hypermyelination is a consequence of additional membrane wraps. The two axons shown are of about equal diameter. (**C**) The size distribution of sciatic nerve axons in adult *Nrg1 type III* transgenic mice ($n = 3$) and wt littermates ($n = 3$) is the same, demonstrating that transgene expression did not cause axonal shrinkage. (**D**) After Nrg1 type III overexpression, reduced *g* ratios were observed for virtually all axons, and changes were more pronounced for smaller caliber axons. Scatter plot displays *g* ratios of individual fibers (obtained from three animals) as a function of the respective axon diameter.

**Neuregulin signals encoding axon caliber.** Whereas glial ErbB receptors are apparently expressed in numerical excess, axonal Nrg1 type III limits myelination. Our data support a model in which the degree of axon-glia signaling constitutes the measure of axon caliber presented to the myelin-forming Schwann cells. This conclusion is compatible with a function of axonal Nrg1 type I at the neuromuscular junction (*32*), severely perturbed myelination in mice lacking ErbB2 in Schwann cells (*17*), and the failure of cultured Schwann cells to myelinate axons from Nrg1 type III knock-out mice (*33*).

Nrg1 action is context dependent, being modified by integrin signaling (*34*). This may explain why Nrg1 overexpression causes hypermyelination in vivo (this study), but when added to cultured Schwann cells Nrg1 induces demyelination and cell death (*35*).

Schwann cells differentiation depends on the phophatidyl-inositol-3-phosphate (PI3) kinase and Akt pathway downstream of activated ErbB2/3 receptors (*36*, *37*). In our working model, phosphorylated lipids generated by PI3 kinase at the adaxonal membrane diffuse through myelin membranes to reach the Schwann cell soma. Alternatively, signaling intermediates could travel to the perinuclear cytoplasm through Schmitt-Lantermann incisures or radial gap junctions (*38*).

An important future goal is to understand how neurons regulate Nrg1 expression as a function of their own axonal dimension. Also other axonal proteins, including sodium and potassium channels (*1*), require axon size– and length-dependent gene regulation. It is intriguing that the Nrg1 C-terminal domain can be proteolytically cleaved to become a signaling molecule itself (*39*). Whether this cleavage contributes to a back-propagation of axonal size information remains to be determined.

## References and Notes


1. S. G. Waxman, *Curr. Biol.* **7**, R406 (1997).
2. S. G. Waxman, *Muscle Nerve* **3**, 141 (1980).
3. H. H. Donaldson, G. W. Hoke, *J. Comp. Neurol.* **15**, 1 (1905).
4. R. L. Friede, R. Bischhausen, *Brain Res.* **235**, 335 (1982).
5. R. L. Friede, *Exp. Neurol.* **92**, 234 (1986).
6. J. P. Fraher *et al.*, *Acta Neuropathol.* **79**, 364 (1990).
7. P. L. Williams, C. P. Wendell-Smith, *J. Anat.* **109**, 505 (1971).
8. E. Pannese *et al.*, *Anat. Embryol.* **175**, 423 (1987).
9. T. Voyvodic, *Nature* **342**, 430 (1989).
10. G. A. Elder, V. L. Friedrich, R. A. Lazzarini, *J. Neurosci. Res.* **65**, 493 (2001).
11. D. L. Falls, *Exp. Cell Res.* **284**, 14 (2003).
12. M. Gassmann, G. Lemke, *Curr. Opin. Neurobiol.* **7**, 87 (1997).
13. Y. Yarden, M. X. Sliwkowski, *Nat. Rev. Mol. Cell Biol.* **2**, 127 (2001).
14. A. Buonanno, G. D. Fischbach, *Curr. Opin. Neurobiol.* **11**, 287 (2001).
15. K. Adlkofer, C. Lai, *Glia* **29**, 104 (2000).
16. A. N. Garratt, S. Britsch, C. Birchmeier, *Bioessays* **22**, 987 (2000).
17. A. N. Garratt, O. Voiculescu, P. Topilko, P. Charnay, C. Birchmeier, *J. Cell Biol.* **148**, 1035 (2000).
18. G. Lemke, *Mol. Cell. Neurosci.* **7**, 247 (1996).
19. D. Meyer *et al.*, *Development* **124**, 3575 (1997).
20. W. H. Ho, M. P. Armanini, A. Nuijens, H. S. Phillips, P. L. Osheroff, *J. Biol. Chem.* **270**, 14523 (1995).
21. D. Wolpowitz *et al.*, *Neuron* **25**, 79 (2000).
22. Materials and methods are available as supporting material on *Science* Online.
23. O. Bermingham-McDonogh, Y. T. Xu, M. A. Marchionni, S. S. Scherer, *Mol. Cell Neurosci.* **10**, 184 (1997).
24. G. V. Michailov *et al.*, unpublished data.
25. M. Sereda *et al.*, *Neuron* **16**, 1049 (1996).
26. C. Rosenbaum *et al.*, *Exp. Neurol.* **148**, 604 (1997).
27. P. Caroni, *J. Neurosci. Methods* **71**, 3 (1997).
28. F. H. de Webster, *Neurosci. Res. Program Bull.* **9**, 470 (1971).
29. B. G. Brinkmann *et al.*, unpublished data.
30. J. M. Cosgaya, J. R. Chan, E. M. Shooter, *Science* **298**, 1245 (2002).
31. J. H. O'Neill, J. M. Jacobs, R. W. Gilliatt, M. Babs, *Acta Neuropathol.* **63**, 313 (1984).
32. W. Sandrock *et al.*, *Science* **276**, 599 (1997).
33. J. Salzer, personal communication.
34. H. Colognato *et al.*, *Nat. Cell Biol.* **4**, 833 (2002).
35. G. Zanazzi *et al.*, *J. Cell Biol.* **152**, 1289 (2001).
36. P. Maurel, J. L. Salzer, *J. Neurosci.* **20**, 4635 (2000).
37. K. B. Citri, *Exp. Cell Res.* **284**, 54 (2003).
38. R. J. Balice-Gordon, L. J. Bone, S. S. Scherer, *J. Cell Biol.* **142**, 1095 (1998).
39. J. Bao, D. Wolpowitz, L. W. Role, D. A. Talmage, *J. Cell Biol.* **161**, 1133 (2003).


40. We thank E. Nicksch and A. Fahrenholz for excellent technical help, J. Archelos (Graz) for providing us with P0 antibodies, S. S. Scherer (Pennsylvania) for advice on teased-fiber preparations, J. Salzer (New York) for helpful comments on the manuscript, and members of the Nave lab for discussion. This work was supported by the Deutsche Forschungsgemeinschaft (SFB523), the Hertie Institute of Multiple Sclerosis Research, and by grants of the European Union (to K.-A.N.). M.W.S. was supported in part by the Departments of Clinical Neurophysiology and Neurology at the University of Göttingen, and M.H.S., by the National Multiple Sclerosis Society.


**Supporting Online Material**

www.sciencemag.org/cgi/content/full/1095862/DC1
Materials and Methods
Figs. S1 to S7
References and Notes


21 January 2004; accepted 8 March 2004
Published online 25 March 2004;
10.1126/science.1095862
Include this information when citing this paper.